Adeno-associated virus type 2-mediated gene transfer of a short hairpin-RNA targeting human IGFBP-2 suppresses the proliferation and invasion of MDA-MB-468 cells

CHAO GAO[1], RU-SONG ZHANG[2], NAN ZHENG[3] and CHEN WANG[3]

[1]The Center for Clinical Reproductive Medicine, Jiangsu Hospital, Nanjing, Jiangsu 210029;
[2]The Pathology Department, Nanjing General Hospital of Nanjing Military Command, Nanjing, Jiangsu 210002;
[3]State Key Laboratory of Chemistry for Life Science & Jiangsu Key Laboratory of Molecular Medicine, Medical School of Nanjing University, Nanjing, Jiangsu 210093, P.R. China

Received March 3, 2017; Accepted August 14, 2017

DOI: 10.3892/mmr.2018.8434

Abstract. Adeno-associated virus 2 (AAV2) is prepotent in the biological treatment of breast tumor because of its low pathogenicity and immunogenicity. Our previous study demonstrated that insulin-like growth factor-binding protein 2 (IGFBP-2) was highly expressed in patients with breast metastasis. In the present study, the effects of recombinant AAV2 on the growth and metastasis of breast cancer cells were determined *in vitro*, and *in vivo*. rAAV2-ZsGreen-shRNA-scramble and rAAV2-ZsGreen-shRNA-hIGFBP-2 were used to transfect MDA-MB-468, and MCF-10A cells respectively, and observed that these virus could not penetrate the normal human breast epithelia MCF-10A cell line. To investigate the effect of the recombinant virus on chemotherapeutics, paclitaxel was added to MDA-MB-468 cells and it was demonstrated that rAAV2-ZsGreen-shRNA-hIGFBP-2-infected MDA-MB-468 cells were highly chemosensitive to paclitaxel compared with rAAV2-ZsGreen-shRNA-scramble-injected cells. In addition, it was demonstrated that the invasive ability of rAAV2-ZsGreen-shRNA-hIGFBP-2-infected MDA-MB-468 cells was highly impaired compared with the rAAV2-ZsGreen-shRNA-scramble group. In the nude mice xenografts, the rAAV2-ZsGreen-shRNA-hIGFBP-2 injection inhibited tumor growth and Ki-67 expression was significantly downregulated compared with the scramble group. Following IGFBP-2 knockdown using rAAV2-ZsGreen-shRNA-hIGFBP-2, matrix metalloproteinase-2 expression was significantly reduced in tumor tissues compared with that in rAAV2-ZsGreen-shRNA-scramble treated tumor tissues. These findings have provided a direction for the application of novel AAV2-based therapeutics for treating aggressive triple-negative breast cancer types.

Correspondence to: Mrs. Chen Wang, State Key Laboratory of Chemistry for Life Science & Jiangsu Key Laboratory of Molecular Medicine, Medical School of Nanjing University, 22 Han Kou Road, Nanjing, Jiangsu 210093, P.R. China
E-mail: wangchen922@nju.edu.cn

Abbreviations: IGFBP-2, insulin-like growth factor-binding protein-2; AAV2, adeno-associated virus type 2; ER, estrogen receptor; PR, progesterone receptor; shRNA, short hairpin ribonucleic acid; HER2, human epidermalgrowth factor receptor-2; DMEM, Dulbecco's modification of Eagle's medium; FBS, fetal bovine serum; MMP-2, matrix metalloproteinase 2; CK-7, cytokeratin-7; MTT, Methylthiazolyldiphenyl-tetrazolium bromide; GAPDH, glyceraldehyde phosphate dehydrogenase; OCT, optimal cutting temperature; PBS, phosphate-buffered saline

Key words: AAV2, MDA-MB-468 cells, breast cancer, tumor xenografts, tumor growth, invasion ability

Introduction

Serum levels of insulin-like growth factor-binding protein-2 (IGFBP-2) are significantly increased in, and have been correlated with, tumor progression in a number of different cancers, including colon (1), ovarian (2,3), lung (4), and prostate (5,6). In addition, the levels of IGFBP-2 in the serum and tumors of breast cancer patients are significantly elevated (7,8), and tumor IGFBP-2 expression correlates with malignancy (7). IGFBP-2 has also been shown to modulate cell adhesion and migration (9) in an IGF-independent manner, but the exact nature of its role in breast cancer is not clear. IGFBP-2 contains an arginine-glycine-aspartic(RGD) integrin-recognition sequence near its C-terminus. Accordingly, the biological effects of this protein are reported to be mediated by its ability to bind to integrin receptors such integrin-$\alpha5\beta1$, thereby facilitating activation of downstream signaling pathways (9,10). Our previous work has demonstrated that adipocytes surrounding breast cancer cells may secrete IGFBP-2 and promote breast cancer metastasis (11). We have also found that IGFBP-2 expression was elevated in both cancer cells and adipocytes in patients presenting with metastatic breast disease. In this study, we have designed an adeno-associated virus (AAV) construct containing a small interfering RNA to IGFBP-2 to examine the function of this protein in MDA-MB-468 cells. These cells are a model of

triple-negative ($ER^-/PR^-/HER2^-$) breast cancer and have high basal levels of IGFBP-2 expression.

AAVs are attractive candidates for the creation of viral vectors for gene therapy, as these viruses are non-pathogenic and less immunogenic compared to other gene therapy vectors (12-15). AAVs are non-enveloped parvoviruses that measure approximately 22 nm in diameter and have been used in many clinical trials for cancer treatment (16). In addition, Alam *et al* have found that although AAV2 is capable of infecting normal human mammary epithelial cells (nHMECs), it is unable to express Rep proteins or undergo active replication in this cell type (17). Therefore, AAV2 maybe a useful candidate for breast cancer gene therapy. Moreover, Alam *et al* have also found that infection with wild-type adeno-associated virus type2 (AAV2) inhibited proliferation of breast cancer cell lines representing both weakly (MCF-7 and MDA-MB-468) and highly invasive (MDA-MB-231) cancer types (17). Therefore, the present study evaluated the effects of a recombinant AAV2(rAAV2) encoding an shRNA to human IGFBP-2 (rAAV2-shRNA-hIGFBP-2) on phenotypes of MDA-MB-468 breast cancer cells. We show that administration of rAAV2-shRNA-hIGFBP-2 resulted in down-regulation of IGFBP-2 *in vitro* and inhibited MDA-MB-468 breast cancer cell proliferation. Since paclitaxel is a commonly used drug to treat human breast cancer patients with metastasis and the drug resistance has limited its use, our tests show that rAAV2-shRNA-hIGFBP-2 could enhance the effect of paclitaxel at the same concentration. We also demonstrate that MCF10A cells are resistant to rAAV2-shRNA-scramble infection and *in vivo* injection of rAAV2-shRNA-hIGFBP-2 inhibits the growth of tumor xenografts derived from MDA-MB-468 cells. Finally, we show that rAAV2-shRNA-hIGFBP-2 can reduce the invasive potential of MDA-MB-468 cells to some extent.

In breast cancer, autocrine or paracrine IGFBP-2 signaling may be an important event during metastasis and drug resistance (18), thereby making this molecule an attractive target for therapeutic intervention. To this end, the present study seeks to improve the clinical feasibility of therapies that target IGFBP-2 using a relatively safe viral vector: Adeno-associated virus 2.

Materials and methods

Ethics statement. The study was approved by the institutional review board (CWO) of Medical School of Nanjing University (Nanjing, China). All experimental procedures were conducted in conformity with institutional guidelines for the care and use of laboratory animals.

Cell culture and infection with recombinant AAV2. The adenoviral packaging 293T/17 cell line (ATCC#CRL-11268), as well as the MCF-7 (ATCC#HTB-22), SKBR-3 (ATCC#HTB-30), MDA-MB-231 (ATCC#HTB-26) and MDA-MB-468 (ATCC #132) human breast cancer cell lines originated from the American Type Culture Collection (ATCC, Manassas, VA, USA). MCF-10A cells were purchased from Shanghai Baili Biotechnology Ltd (Baili, Shanghai, China). MDA-MB-468 cells were maintained in Leibovitz's L-15 medium (GIBCO) and the remaining cell lines were maintained in high-glucose Dulbecco's Modified Eagle Medium (DMEM, GIBCO) supplemented with 110 mg/l sodium pyruvate, 2 mg/l pyridoxine hydrochloride, 2 g/l sodium bicarbonate, 10% FBS, penicillin (100 U/ml) and streptomycin (100 mg/ml). All cell cultures were maintained at 37˚C in 5% CO_2. MDA-MB-468 cells were grown to approximately 80% confluence before infection with adenovirus. Specifically, culture medium was aspirated from the plates, and infections were conducted using rAAV2-ZsGreen-shRNA-scramble or rAAV2-ZsGreen-shRNA-hIGFBP-2 (our laboratory cooperated with Shenzhen Biowit Technologies Company) in serum-free L-15 medium at an optimized concentration of $1.5x10^{11}$ viral genomes/ml (vg/ml). Mock infections were also performed using only serum-free L-15 medium. Plates were incubated at 37˚C for 12 h with intermittent agitation. At the end of the incubation, residual medium was aspirated from the plates and replaced with fresh L-15 medium supplemented with 10% serum. Infected cells were then stimulated with paclitaxel or IGFBP-2 on the fourth day after infection, and total RNA or protein were collected at this time. Fluorescent micro-graphs were also obtained at this time point using a Nikon TE 2000 microscope (magnification x100) to confirm infection efficiency.

Preparation of AAV2-ZsGreen virus carrying short hairpinRNA targeting human IGFBP-2. The pAAV-ZsGreen-shRNA plasmid was supplied by Biowit Technologies (Shenzhen, China). The 68 bp shRNA template sequences were designed and synthesized as follows: hIGFBP2-F: 5'-GATCCGGAGCAGGTTGCAGACAATTTCAAGAGAATTGTCTGCAACCTGCTCCTTTTTTAGATCTA-3'; hIGFBP2-R: 5'-AGCTTAGATCTAAAAAAGGAGCAGGTTGCAGACAATTCTCTTGAAATTGTCTGCAACCTGCTCCG-3'; hScramble-F: 5'-GATCCGCTCGCCTGTCTACTAACTAATTCAAGAGAATTGTCTGCAACCTGCTCCTTTTTTAGATCTA-3'; hScramble-R: 5'-AGCTTAGATCTAAAAAAGGAGCAGGTTGCAGACAATTCTCTTGAATTAGTTAGTAGACAGGCGAGCG-3'. BamHI and HindIII restriction sites were used for cloning. An equimolar mixture of the sense and anti-sense shRNA templates were denatured by boiling and were annealed at the speed of 5˚C/h to 20˚C in a thermocycler to form double-stranded DNA. The purified products were then directly inserted between BamHI and HindIII restriction sites downstream of the hU6 promoter in the pAAV-ZsGreen-shRNA vector. The final recombinant plasmids were named, 'pAAV-ZsGreen-shRNA-hIGFBP2' and 'pAAV-ZsGreen-shRNA-hScramble,' and were verified by restriction enzyme digestion and sequencing at Shanghai SANGON Biological Engineering Technology and Service Co, Ltd. Adenoviral packaging 293T/17 cells were transfected with pAAV-ZsGreen-shRNA-hIGFBP2 or pAAV-ZsGreen-shRNA-hScramble together with pAAV-RC and pAAV-Helpervia modified calcium phosphate co-precipitation when cell monolayers were 50-60% confluent. The cells were harvested after 72 h of transfection, and re-suspended in cell lysis buffer (10 mM Tris-HCl, pH 8.5, 150 mM NaCl). Next, the cells were frozen and thawed three times in liquid nitrogen and at 37˚C, respectively. The lysate was then centrifuged at 4,000 x g for 10 min, and the supernatant was collected. Next, solid NaCl and PEG-8000

were added to the supernatant to final concentrations of 1 M and 10% (w/v), respectively, and the mixture was agitated to dissolve these components during a 1 h incubation on ice. After a 15 min centrifugation at 9,000 x g, the pellet was mixed with 1.38 g/ml of CsCl and centrifuged at 500,000 x g for 24 h at 4˚C to isolate the rAAV2-ZsGreen-shRNA viral particles. Determination of viral titer was performed via qPCR amplification for purified rAAV2 and was calculated at $5x10^{12}$ vg/ml.

MTT assay. MDA-MB-231 and MCF-7 cells were cultured in 96-well plates and were serum-starved for 24 h when they reached 70% confluency. Next, culture medium with 5% FBS was added to the cells, supplemented with either 50 μM paclitaxel alone, or both 50 μM paclitaxel and 100 ng/ml IGFBP-2. To avoid attenuation the effect of IGFBP-2, cells were treated with IGFBP-2 a second time 24 h after the initial exposure. Cell viability was then determined both 48 and 72 h following drug treatment using the3-(4,5-dimethylthiazol-2-yl)-2,5-dip henyltetrazoliumbromide (MTT) assay (Sigma). Briefly, the cells were incubated with a 0.5% MTT solution (diluted in culture medium) for 4 h. Then 100 μl of a 0.04 M dimethylsulfoxide solution were added to each well, followed by incubation at 37˚C for an additional 4 h. The absorbance of the reaction product was measured at 570 nm and is proportional to cell viability. The data were expressed as the mean ± S.D. and were used to generate growth curves. Each treatment group was assayed in triplicate.

Trypan blue cell counting. After infection with $1.5x10^{11}$ vg/ml rAAV2-ZsGreen-shRNA-scramble or AAV2-ZsGreen-shRNA-hIGFBP-2 for four days, MDA-MB-468 cells were switched to growth medium containing 5% serum and were treated with paclitaxel or vehicle control for 24 h. For each experiment, all treatments were performed in triplicate, and each experiment was repeated at least three times. Both attached and floating cells were collected by centrifugation and were stained with 0.04% Trypan blue. The number of viable and non-viable cells was quantified with a hemocytometer, and dead cells were divided by all cell counts (18).

Cell invasion assays. After infection with $1.5x10^{11}$ vg/ml rAAV2-ZsGreen-shRNA-scramble or rAAV2-ZsGreen-shRNA-hIGFBP-2 for 4 days, or stimulation with 100 ng/ml IGFBP-2 for 24 h alone, MDA-MB-468 cells were trypsinized and re-suspended in serum-free culture medium. The upper chambers of Transwell inserts (8.0 μm membrane pores, Costar, USA) were subsequently coated with 2.5 mg/ml Matrigel (LOT: 356234, BD Biosciences, USA) and incubated at 37˚C for 30 min. A total of 10^5 cells in 200 μl of medium were then added to the upper chambers of the inserts and were allowed to migrate toward the bottom chambers, which contained medium with 20% FBS as a chemoattractant. After 24 h, the cells on the apical surfaces of the membranes were removed using a cotton swab, and cells on the underside were fixed in 3.7% paraformaldehyde (PFA) and stained with crystal violet. Quantification of migrated cells was performed by dissolving crystal violet with 10% acetic acid, and the optical density of each sample was read with a micro-plate reader at 595 nm. Phase contrast micro-graphs were also obtained at a magnification of x100. Experiments were performed with technical duplicates and were repeated at least three times with consistent results.

Western blotting and immunohistochemistry. When MDA-MB-231, MDA-MB-468, MCF-7 and SKBR-3 cells reached approximately 60-70% confluence in their conventional growth media, they were then switched to either serum-free medium containing 100 ng/ml IGFBP-2, or serum-free medium alone. Protein was collected after 24 h. Protein from MDA-MB-468 cells infected with AAV2 was harvested four h after infection. Western blotting was performed according to established protocols (19), and the following antibodies were used: IGFBP-2 (1:1,000, Abcam4243), ER-a (1:1,000, sc-73479), integrin-α5β (1:1,000, sc-10729), p-ErbB2 (1:1,000, CST#2241), ErbB2 (1:1,000, CST#2242) and GAPDH (1:1,000, BD Biosciences). Immunohistochemical staining was performed on 5 μm formalin-fixed, paraffin-embedded tumor tissue sections. Tissue sections were deparaffinized in xylenes and hydrated in a graded sequence of ethanol solutions. For antigen retrieval, sections were then heated in a microwave in citrate buffer (pH 6.0). After cooling, nonspecific binding was blocked with diluted serum (5% bovine serum albumin) followed by incubation with antibodies against CK-7 (1:500, Abcam 183344), IGFBP-2 (1:300, Abcam 109284), MMP-2 (1:500, Abcam 1818) and Ki67 (1:1,000, Abcam 92742) at room temperature in a humidified chamber for 2 h. Negative control sections incubated without primary antibodies were also used. After incubation with primary antibodies, sections were washed with phosphate-buffered saline (PBS) and subsequently treated using the corresponding biotinylated secondary antibody from an Ultravision ONE kit (Thermo Fisher Scientific, USA) according to the manufacturer's protocol. Peroxidase activity was visualized using 3,3'-diaminobenzidine, and sections were counterstained with hematoxylin.

Detection of IGFBP-2 gene expression. MDA-MB-231, MDA-MB-468, MCF-7 and SKBR-3 cells were stimulated with 100 ng/ml IGFBP-2 for 24 h in serum-free medium, and total cell RNA was extracted using TRIzol reagent (Invitrogen) according to the manufacturer's instructions. Total viral RNA from infected MDA-MB-468 and MCF-10A cells was also extracted. RNA yields were measured using a NanoDrop D-2000 (Thermo Fisher Scientific, USA) instrument. First-strand cDNA was then synthesized from 1 μg total RNA using oligo-dT rimers and the SuperScript II Reverse Transcriptase kit (Invitrogen), according to the manufacturer's instructions. Quantitative real-time PCR was performed in 20 μl reaction mixtures containing 1 μl of the cDNA preparation, 10 μl 2X SYBR Green Premix Ex Taq (Takara, DRR041S), and 1 μM primer pairs on an ABI Step One PCR Instrument. The primer sequencesused for IGFBP-2 amplification were R: 5-GTCTACTGCATCCGCTGGGT-3; F: 5-GCAAGGGTGGCAAGCATC-3, and the primer sequences used for GAPDH amplification were R: 5-GGAAGATGG TGATGGGATT-3; F: 5-AACGGATTTGGTCGTATTG-3. The thermal profile for the real-time PCR reaction consisted of 5 min at 95˚C followed by 40 cycles of 30 sec at 95˚C and 1 min at 60˚C. Each sample was assayed in triplicate. Threshold values were determined for each sample/primer pair, and the average and standard error of gene expression were calculated. The specificity of the PCR products was then verified by melt curve

analysis, and products from each reaction were electrophoresed on a 1.8% agarose gel. GAPDH was used as an internal standard for mRNA expression.

rAAV2-ZsGreen-shRNA-hIGFBP-2 in breast cancer hypodermic model. The effect of rAAV2-ZsGreen-shRNA-hIGFBP-2 on breast tumor growth was determined using the athymic mouse model of breast cancer by hypodermic injection. Female BALB/c nude mice used in this study (4-5 weeks old and weighing 20.0±2.0 g) were obtained from the Changzhou Vince Experimental Animal Co. Ltd (Qualification certificate numbers: 201505694 and 201508683) and were housed in a defined pathogen-free environment. All procedures were approved by the National Animal Care and Use Committee in China and the Laboratory Animal Center of the Academy of Medical Sciences of Nanjing University. Briefly, MDA-MB-468 cells were trypsinized and washed with serum-free L-15 medium three times to remove residual enzyme. Next, mice were anesthetized via inhalation of isoflurane, and 10^7 MDA-MB-468 cells in 100 μl of a mixture consisting of 50 μl complete medium and 50 μl Matrigel (BD, 356234) were injected subcutaneously into the left flank. After the tumor volume reached approximately 75^3 mm (around the 15th day post-injection), AAV2-ZsGreen-shRNA-hIGFBP-2 or scramble viral particles ($1.0x10^8$ vg/ml in PBS) were administered by direct injection into the xenograft (4 sites/lump, 25 μl/site) using a syringe with a 30-gauge needle every five days for 30 days. A control group of mice received intratumoral injections of PBS in parallel with the treatment groups. Tumor dimensions were measured with vernier calipers every five days beginning at the 15th day post-injection by euthanatizing three mice and excising their tumors. Tumor volumes were calculated using the following formula: volume (V) = L x W2 x π/6, where L is the length and W is the width of the tumor. For histological analysis, subcutaneous tumors were excised and fixed in 4% paraformaldehyde for 12 h and embedded in paraffin. Additionally, frozen tumor tissue was embedded in optimal cutting temperature (OCT) compound, and sectioned into 6 μm sections with a freezing microtome. The infection efficiency of *in vivo* viral gene transfer was assessed in cryosectioned tumor tissue using fluorescence microscopy (wave length 488 nm).

Statistical analysis. Results are expressed as means ± standard deviation (SD). Differences between the groups were determined with the Student's t-test. All analyses were performed with SPSS software (IBM, USA), version 10.0. Differences among groups were considered to be significantly different at $P<0.05$.

Results

IGFBP-2 promoted survival and impacted chemosensitivity of breast cancer cells . Exogenous addition of IGFBP-2 increased the protein-level expression of IGFBP-2 and integrin-α5β1 in MDA-MB-231, MDA-MB-468, MCF-7 and SKBR-3 cells, which represent different subtypes of breast cancer (Fig. 1A). Among these cell lines, the triple-negative breast cancer cell line, MDA-MB-468, exhibited the most robust levels of basal IGFBP-2 expression (Fig. 1A). In addition, exogenous IGFBP-2 (100 ng/ml) enhanced the viability of paclitaxel-treated MDA-MB-231 and MCF-7 cells (Fig. 1B and C), although no further increases in survival were observed when the dose of IGFBP-2 was increased to 500 ng/ml. Moreover, IGFBP-2 was down-regulated on the fourth day after infection with rAAV2-ZsGreen-shRNA-hIGFBP-2. By the fifth day after infection, loss of IGFBP-2 significantly increased the number of dead MDA-MB-468 cells compared to control cells infected with rAAV2-ZsGreen-shRNA-scramble. With respect to chemosensitivity, MDA-MB-468 cells infected with rAAV2-ZsGreen-shRNA-hIGFBP-2 exhibited a greater paclitaxel sensitivity compared to cells infected with rAAV2-ZsGreen-shRNA-scramble. Indeed, the number of dead cells infected with rAAV2-ZSGreen-shRNA-hIGFBP-2 increased to 56% of the total cell population, a 1.9-fold increase over the scramble control (Fig. 1D). Maximal responses to IGFBP-2 knockdown were obtained when viral titers of $1.5x10^{11}$ vg/ml were used.

rAAV2-ZsGreen-shRNAs did not infect normal human mammary epithelial cells MCF-10A. MDA-MB-468 and MCF-10A cells were infected with rAAV2-ZsGreen-shRNA-scramble or rAAV2-ZsGreen-shRNA-hIGFBP-2 at the same viral titers. On the fourth day post-infection, MDA-MB-468 cells exhibited robust green fluorescence, while MCF-10A cells were only weakly fluorescent (Fig. 2A). In addition, MDA-MB-468 cells infected with rAAV2-ZsGreen-shRNA exhibited reduced proliferation, which eventually culminated in apoptosis. These responses were not observed in MCF-10A cells (data not shown). Next, IGFBP-2 expression in MDA-MB-468 but not MCF-10A cells was demonstrated to be down-regulated at both the mRNA and protein levels following infection with rAAV2-ZsGreen-shRNA-hIGFBP-2 (Fig. 2B and C). These results suggest that AAV2 can specifically targeting breast cancer cells, but not normal mammary epithelial cells.

rAAV2-ZsGreen-shRNA inhibited proliferation of MDA-MB-468 cells in vivo. We next asked if direct injection of rAAV2-ZsGreen-shRNA into tumor xenografts could inhibit their growth *in vivo*. To this end, we injected a mixture of MDA-MB-468 cells and Matrigel into the mammary fat pads of nude mice. Fifteen days or 45 days after injection, the mice were euthanized and the tumors were excised (Fig. 3A). Hematoxylin and eosin (H&E) staining was then performed to verify the morphology of the tumor cells. We also used frozen tissue sections to confirm that the viruses had successfully targeted the tumor cells (Fig. 3B). With respect to tumor volume, tumors injected with rAAV2-ZsGreen-shRNA-scramble and rAAV2-ZsGreen-shRNA-hIGFBP-2 both exhibited significantly reduced primary tumor volume compared to control tumors injected with PBS (Fig. 3C), but rAAV2-ZsGreen-shRNA-hIGFBP-2 had more marked effect. In addition, immunohistochemical staining revealed that injection of rAAV2-ZsGreen-shRNA-scramble and rAAV2-ZsGreen-shRNA-hIGFBP-2 both decreased tumor Ki-67 expression (Fig. 3D). A general post mortem examination revealed no obvious organ-specific toxicity in any of the virus-treated animals.

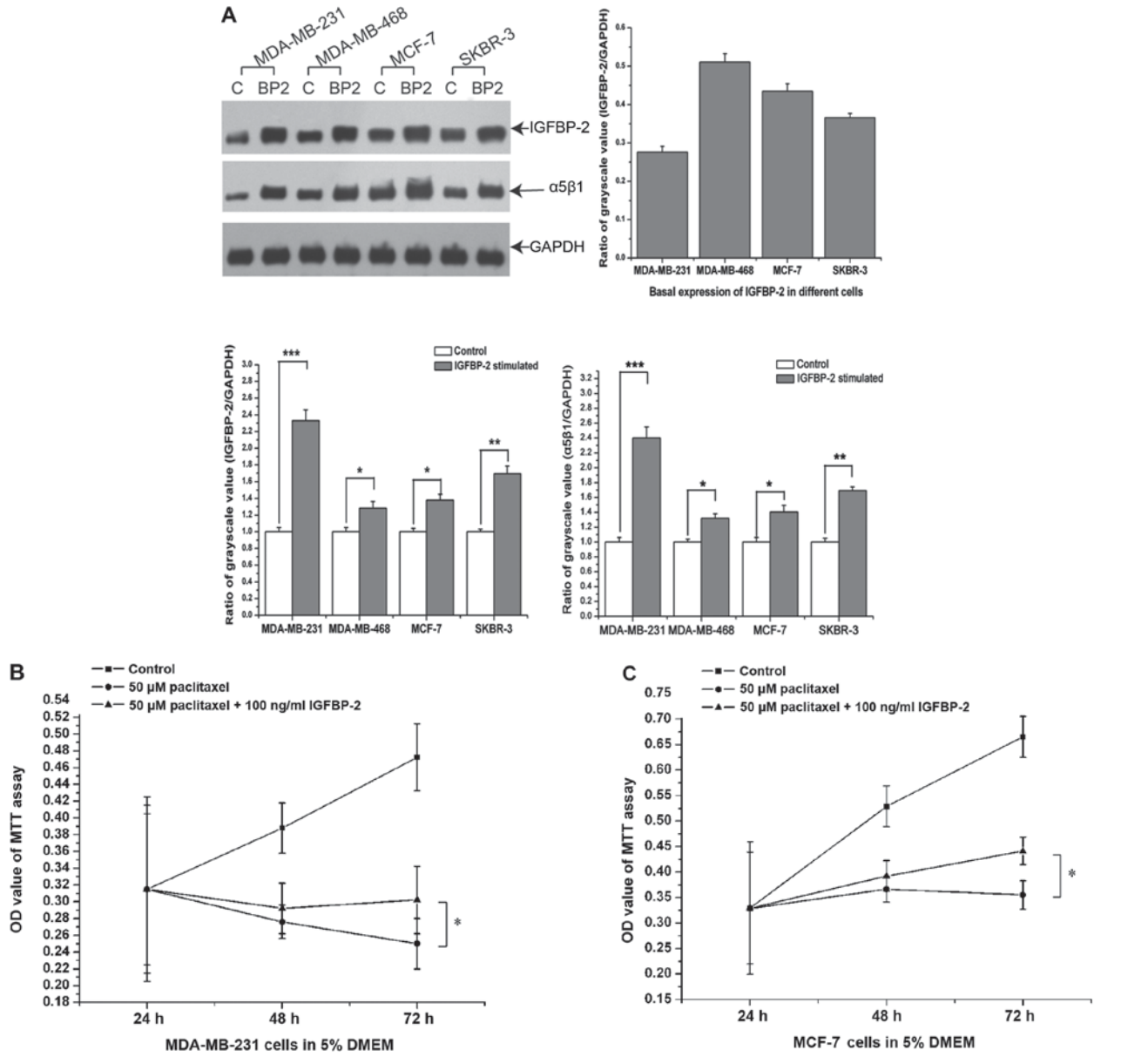

Figure 1. Effects of exogenous IGFBP-2 in four established breast cancer cell lines (A) Exogenous 100 ng/ml IGFBP-2 for 24 h promotes protein-level expression of endogenous IGFBP-2 and integrin-α5β1 in MDA-MB-231, MDA-MB-468, MCF-7 and SKBR-3 with $1.5x10^6$ cells for each sample. At the same time, MDA-MB-468 cells exhibited the most abundant levels of basal IGFBP-2 expression in the immunoblot test. Quantification of IGFBP-2 and integrin-α5β1 expression were detected by Image J software and normalized to GAPDH. We normalized the expression ratios from the control group to 1, and differences in the ratios of the remaining groups were analyzed for statistical significance using Student's t-test (*P<0.05, **P<0.0 1, ***P<0.001). The experiments were repeated for four times. (B) Exogenous 100 ng/ml IGFBP-2 promotes the survival of 50 μM paclitaxel-treated MDA-MB-231 cells. The experiments were performed in three-duplicated wells in 96-well plates and repeated for three times. The error bars indicated the S.D of mean values (**P<0.05). The difference between IGFBP-2 + paclitaxel treatment and paclitaxel alone was *P<0.1. (C) Exogenous 100 ng/ml IGFBP-2 promotes the survival of 50 μM paclitaxel-treated MCF-7 cells. The experiments were performed in three-duplicated wells in 96-well plates and repeated for three times. The error bars indicated the SD of mean values (**P<0.05). The difference between IGFBP-2 + paclitaxel treatment and paclitaxel alone was *P<0.1. (D) Down regulation of IGFBP-2 by $1.5x10^{11}$ vg/ml AAV2-ZsGreen-shRNA-hIGFBP-2 reduces survival of MDA-MB-468 cells in 6-well plates. After being stained with 0.04% Trypan blue, the non-viable cells showed blue color and were quantified with a hemocytometer. Differences in the frequency of dead cells were computed with Student's t-test (**P<0.0 1). The experiments were repeated for four times.

rAAV2-ZsGreen-shRNA-IGFBP-2 suppressed the invasive potential of MDA-MB-468 cells. While IGFBP-2-stimulated MDA-MB-468 cells showed markedly enhanced invasion potential,rAAV2-ZsGreen-shRNA-hIGFBP-2infectedMDA-MB-468

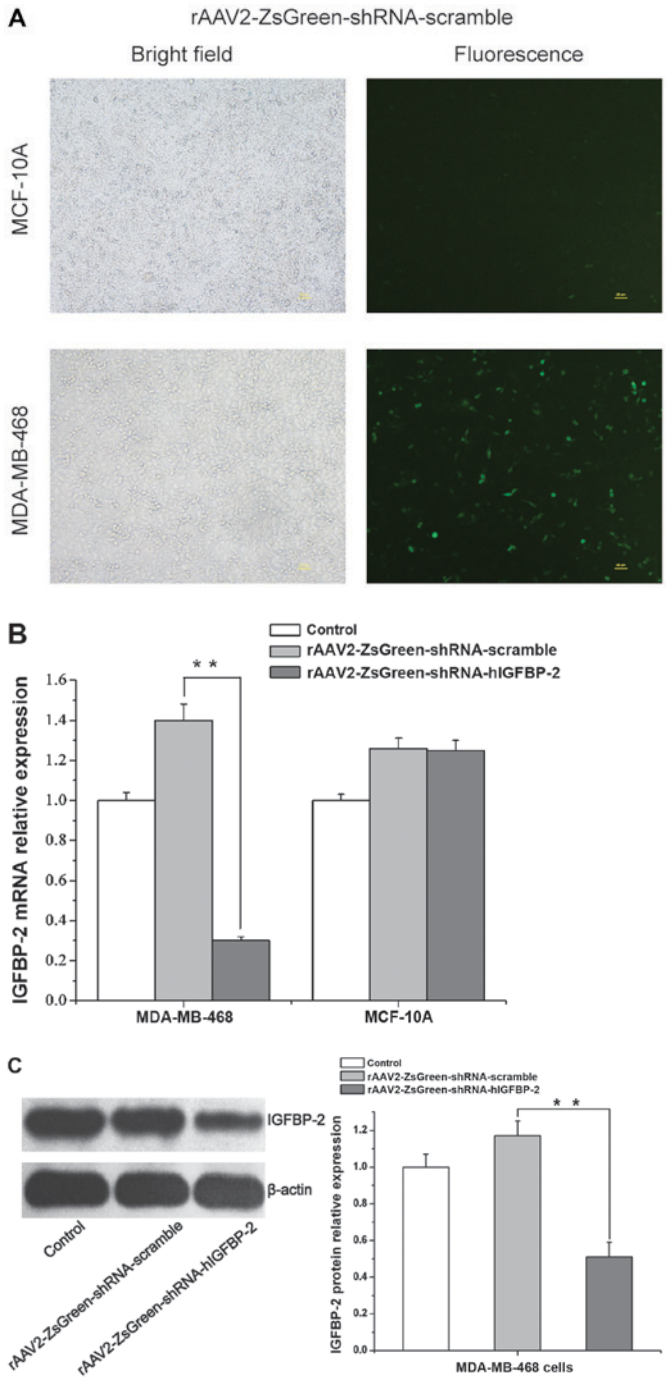

Figure 2. Effects of rAAV2-ZsGreen-shRNA-hIGFBP-2 in MDA-MB-468 and MCF-10A cells. (A) MCF-10A cells are not amenable to rAAV2-ZsGreen-shRNA infection. MDA-MB-468 and MCF-10A cells were infected with rAAV2-ZsGreen-shRNA-scramble at the titer of $1.5x10^{11}$ vg/ml. Images of the same field were taken to show both bright field (cell morphology) and GFP fluorescence (100x). (B) Reverse transcription quantitative PCR was used to quantify IGFBP-2 gene expression levels in MDA-MB-468 and MCF-10A cells infected with $1.5x10^{11}$ vg/ml rAAV2-ZsGreen-shRNA-scramble or rAAV2-ZsGreen-shRNA-hIGFBP-2. The expression of IGFBP-2 mRNA in control cells was normalized to 1 ($^{**}P<0.01$). (C) Western blot analysis was used to confirm IGFBP-2 down-regulation at the protein level in MDA-MB-468 cells infected with $1.5x10^{11}$ vg/ml rAAV2-ZsGreen-shRNA-hIGFBP-2. The expression of IGFBP-2 protein in control cells was normalized to 1 ($^{**}P<0.01$).

cells showed impaired invasion potential compared to control cells infected with rAAV2-ZsGreen-shRNA-scramble (Fig. 4A). These results were quantified by dissolving crystal violet with a micro-plate reader (Fig. 4B). Moreover, mouse tumors injected with rAAV2-ZsGreen-shRNA-hIGFBP-2 exhibited markedly reduced MMP-2 expression compared to tumors injected with either PBS or rAAV2-ZsGreen-shRNA-scramble (Fig. 4C).

Discussion

Breast cancer is the most common cancer type in women and is associated with a high mortality rate due to the propensity of this disease to metastasize. Personalized treatment is often recommended based on histological sub-types characterized by the expression of estrogen (ER), progesterone (PR) and Her-2 receptors. Importantly, patients with triple-negative ($ER^-/PR^-/HER2^-$) breast cancer are often faced with the worst prognosis. Previous work has shown that IGFBP-2 can stimulate the proliferation of a number of different cell types, including prostate cancer cells (20), glioma (21), and chondrocytes (22). Our previous work has also found that IGFBP-2 is secreted into the breast cancer micro environment by adipocytes, where by it promotes cancer metastasis. In this study, we attempted to clarify further the effects of IGFBP-2 in breast cancer cells and establish its role as a putative therapeutic target. This hypothesisis further supported by the observation that exogenous IGFBP-2 could promote survival of MDA-MB-231 and MCF-7 breast cancer cells in the presence of paclitaxel, while loss of IGFBP-2 enhanced the chemosensitivity of MDA-MB-468 cells. We had tried doxorubicin to do the same tests in Fig. 1 but there was not significant difference between different treatments.

IGFBP-2 possesses Arg-Gly-Asp integrin-binding motifs and is among the many proteins that interact with integrin-α5β1. This interaction has been reported to be involved in modulating the effects of IGFBP-2 on glioma cell migration and invasion (23). In our study, exogenous IGFBP-2 could promote the protein-level expression of integrin-α5β1 in four breast cancer cell lines. We also found that exogenous IGFBP-2 up-regulated the expression of endogenous IGFBP-2 in our panel of breast cancer cell lines. Similarly, in a study by Sehgal *et al*, IGFBP-2 was shown to up-regulate β-catenin expression in breast cancer cells, which then further enhanced IGFPB-2 expression via a positive-feedback mechanism (24). Therefore, suppressing the effects of IGFBP-2 may help to impede breast cancer progression.

Among the cell lines tested, the highly metastatic, triple-negative breast cancer cell line, MDA-MB-231, exhibited the most significant increase in IGFBP-2 expression. Moreover, exogenous IGFBP-2 promoted the survival of MDA-MB-231 cells, and enhanced the expression of integrin-α5β1 in this cell type. Therefore, although MDA-MB-231 cells do not exhibit high basal expression levels of IGFBP-2, the progression of tumors derived from this cell line may also be impeded by rAAV2-shRNA-IGFBP-2 therapy. Breast tumors in human patients reside in a complex micro environment, which could significantly modulate cancer cell protein expression. Therefore, *in vitro* studies using human cell lines may not fully recapitulate all features of clinical breast tumors. Nevertheless, given that MDA-MB-468 cells exhibit abundant levels of basal IGFBP-2 expression, this cell type represents a favorable breast cancer model in which to test the effects of rAAV2-shRNA-hIGFBP-2 treatment *in vitro* and *in vivo*. In our *in vitro* study, infection of MDA-MB-468 cells with rAAV2-ZsGreen-shRNA-hIGFBP-2

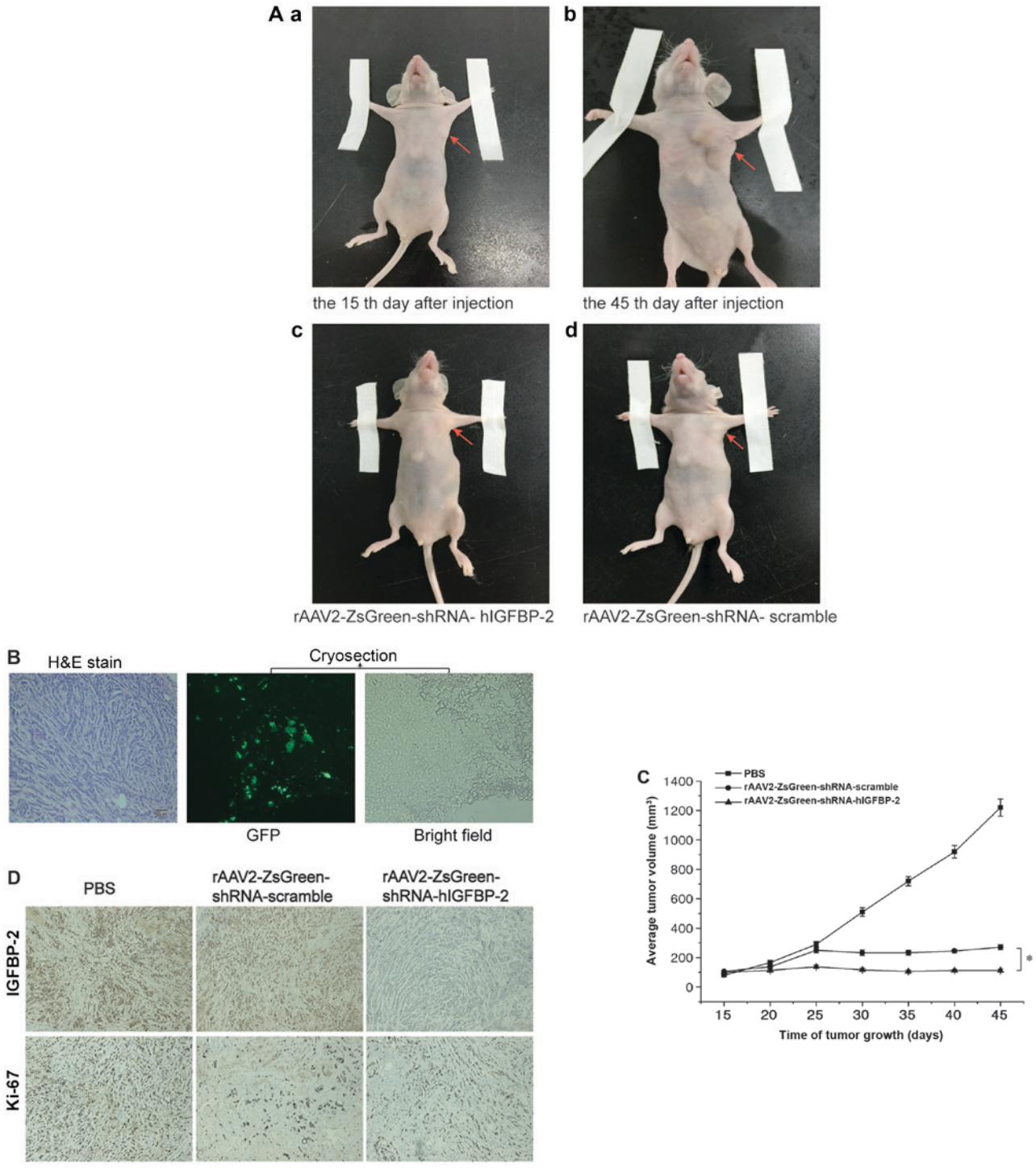

Figure 3. MDA-MB-468 cell-derived tumor xenografts in female nude mice were injected with rAAV2-ZsGreen-shRNA. (A) Representative images of mice injected with MDA-MB-468 cells on (a) the 15th day after injection with 10^7 MDA-MB-468 cells, (b) the 45th day after injection with 10^7 MDA-MB-468 cells. (c) The 45th day after injection with MDA-MB-468 cells, the tumors were injected with rAAV2-ZsGreen-shRNA-hIGFBP-2 every five days. (d) The 45th day after injection with MDA-MB-468 cells, the tumors were injected with rAAV2-ZsGreen-shRNA-scramble every five days. (B) Hematoxylin and eosin staining was used to confirm the morphology of cells in the MDA-MB-468 xenografts (200x). Infection efficiency of *in vivo* virus-mediated gene transfer was assessed by fluorescence microscopy on cryosections. Images of the same field were taken to show both bright field (tissue morphology) and GFP fluorescence (200x). (C) Tumor growth curves were constructed to calculate the growth rates of tumor xenografts. Tumors were injected with PBS, rAAV2-ZsGreen-shRNA-scramble or hIGFBP-2 viral particles on the 15th day after cell injection. The difference between rAAV2-ZsGreen-shRNA-scramble and rAAV2-ZsGreen-shRNA-hIGFBP-2 was $^*P<0.1$. (D) Representative micro-photographs of immunohistochemical staining for IGFBP-2 and Ki-67 in tumor tissue sections obtained on the 45th day after injection with MDA-MB-468 cells (100x). The primary antibodies specifically recognized human epitopes.

led to IGFBP-2 down-regulation, increased cell death and enhanced chemosensitivity to paclitaxel compared to infection with rAAV2-ZsGreen-shRNA-scramble. These results supported the notion that rAAV2-ZsGreen-shRNA-hIGFBP-2 may have therapeutic effects on triple-negative breast cancer cells. Moreover, the inability of AAV2 to infect normal mammary epithelial (MCF-10A) cells renders the potential clinical applications of this therapy even more exciting. Actually

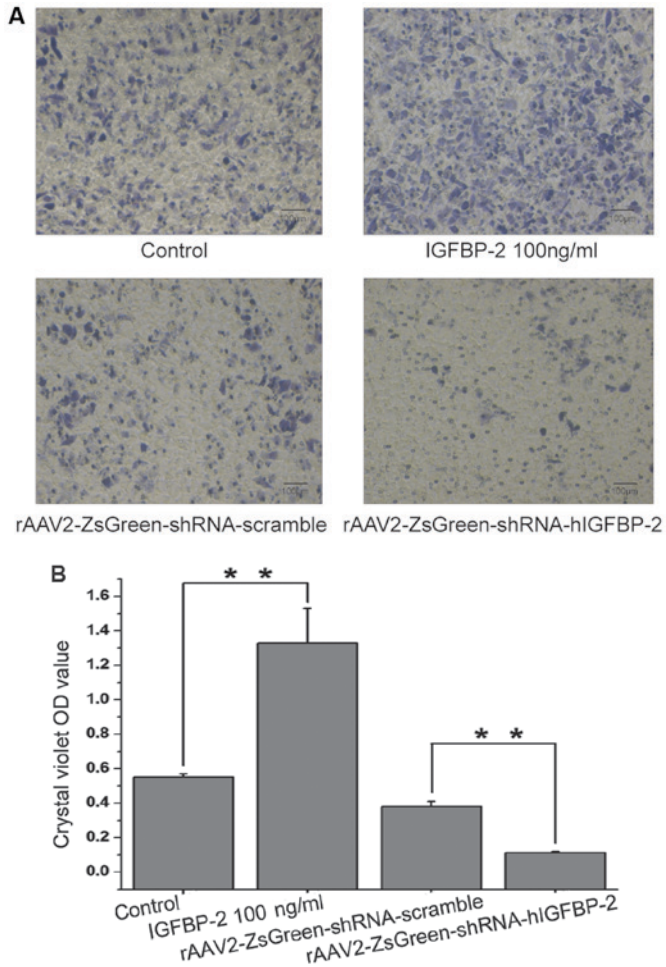

Figure 4. *In vitro* and invo effects of rAAV2-ZsGreen-shRNA-IGFBP-2 on the invasive ability of MDA-MB-468 cells. (A) Exogenous IGFBP-2 enhanced the invasive potential of MDA-MB-468 cells, whereas infection with $1.5x10^{11}$ vg/ml rAAV2-ZsGreen-shRNA-hIGFBP-2 reduced invasion in this cell type. (B) Quantification was performed by dissolving crystal violet in 10% acetic acid, and reading the OD values with a micro-plate reader at 595 nm. Images were taken at 100x magnification. The data shown are the means of triplicate wells, and the error bars represent the S.D ($^{**}P<0.01$). (C) Representative micro-photographs of immunohistochemical staining for MMP-2 in tumor tissue sections obtained on the 45th day after injection with MDA-MB-468 cells (100x). The primary antibodies specifically recognized human epitopes.

AAV2 transfection efficiency was strong in a certain number of breast cancer lines which are not confined to TNBC. We can see evidence based on southern blot analysis that MCF-7 cells with ER(+) can also be transfected with AAV2 in reference (17). In contrast, neither the 4.7 kb replicative form DNA monomer nor the Rep protein expression could be detected in nHMECs. To our knowledge, AAV2 transfection efficiency was strong in human breast cancer cell line MCF-7, MDA-MB-468, MDA-MB-231 and MDA-MB-435. We hope this virus which can not reproduce in normal human epithelial cells may attribute to future clinical therapy of human breast cancer. We speculate that this virus could not replicate in MCF-10A cells because AAV2-encoded Rep proteins may be inhibited by certain factors present in normal mammary epithelial cells.

The clinical application of small interfering RNA (siRNA)-based therapy is limited by the poor stability, poor intracellular uptake, and rapid enzymatic degradation of these molecules. To overcome these limitations, we used adeno-associated virus type 2 (AAV2) to deliver siRNAs to cancer cells. Importantly, this method is non-pathogenic, and these viruses do not infect normal human mammary epithelial cells. Several lines of evidence suggest that over-expression of IGFBP-2 increases cell growth and metastatic potential in several tumor types, including ovarian (25), prostate (26), and bladder cancer (27), as well as glioblastoma (28). Based on the results of our study, we expect that recombinant AAV2-ZsGreen-shRNA-hIGFBP-2-mediated degradation of IGFBP-2 mRNA has significant potential in the treatment of breast cancers characterized by IGFBP-2 over-expression. In addition, Alam *et al* determined that infection of nude mice with wild-type AAV2 induced necrosis and inhibited tumor growth in xenograft models of breast cancer (29). Using a similar mouse model, our study also found that intratumoral injection with $1.0x10^{8}$ vg/ml of rAAV2-ZsGreen-shRNA-scramble or rAAV2-ZsGreen-shRNA-hIGFBP-2 both reduced tumor volume compared to injections of PBS alone, as evidenced by reduced Ki-67 expression. However, the exact mechanism by which AAV2 infection inhibits tumor growth is not known. According to the literature, it is reasonable to predict that the structures of certain AAV2 proteins, such as Rep, may resemble those of eukaryotic cell cycle checkpoint proteins. Accordingly, AAV2-mediated rescue of defective tumor cell checkpoint proteins would greatly down-regulate cell proliferation. Although the specific protein signals downstream of IGFBP-2 have not been identified, the results of this observational study can confirm that rAAV2-ZsGreen-shRNA-hIGFBP-2 can inhibit the proliferation of tumor xenografts derived from MDA-MB-468 cells more significantly.

Furthermore, the rAAV2-ZsGreen-shRNA-hIGFBP-2 -infected MDA-MB-468 cells exhibited reduced invasive potential *in vitro*, whereas exogenous IGFBP-2 stimulated MDA-MB-468 invasion. Taken together, these results further suggest that this recombinant virus maybe a promising method to impede breast cancer cell metastasis. In our *in vivo* study, tumor xenografts injected with rAAV2-ZsGreen-shRNA-hIGFBP-2 exhibited remarkably reduced MMP-2 expression compared to tumors injected with rAAV2-ZsGreen-shRNA-scramble, suggesting that rAAV2-ZsGreen-shRNA-hIGFBP-2 maybe a useful tool for preventing metastasis in breast cancer patients. Importantly, our previous work has demonstrated that exogenous IGFBP-2 could enhance the expression of MMP-2 in breast cancer cells (11). Therefore, this result is in accord with the trans-well assay and indicates that rAAV2-ZsGreen-shRNA-hIGFBP-2 maybe used to impede tumor metastasis in breast cancer patients. Taken together, our *in vitro* and *in vivo* results indicate that rAAV2-ZsGreen-shRNA-hIGFBP-2 can inhibit the growth of MDA-MB-468 cells, as well as enhance chemosensitivity and reduce invasive potential in this cell type.

In conclusion, we have constructed an AAV-2-mediated siRNA delivery system designed to target IGFBP-2-regulated pathways in breast cancer. The effectiveness of this system in both *in vitro* and *in vivo* models has been reported for the first time in the present study. We show that MCF10A cells are resistant to rAAV2-shRNA-scramble infection and *in vivo* injection of rAAV2-shRNA-hIGFBP-2 inhibits the growth of tumor xenografts derived from MDA-MB-468cells. We also demonstrate that rAAV2-shRNA-hIGFBP-2 can reduce the invasive potential of MDA-MB-468cells *in vitro*.

Acknowledgements

This article is supported by the Jiangsu Natural Science Foundation of China (grant no. BK20130591). the authors would like to thank the company Biowit Technologies (Shenzhen, China).

References

1. el Atiq F, Garrouste F, Remacle-Bonnet M, Sastre B and Pommier G: Alterations in serum levels of insulin-like growth factors and insulin-like growth-factor-binding proteins in patients with colorectal cancer. Int J Cancer 57: 491-497, 1994.
2. Karasik A, Menczer J, Pariente C and Kanety H: Insulin-like growth factor-I (IGF-I) and IGF-binding protein-2 are increased in cyst fluids of epithelial ovarian cancer. J Clin Endocrinol Metab 78: 271-276, 1994.
3. Baron-Hay S, Boyle F, Ferrier A and Scott C: Elevated serum insulin-like growth factor binding protein-2 as a prognostic marker in patients with ovarian cancer. Clin Cancer Res 10: 1796-1806, 2004.
4. Lee DY, Kim SJ and Lee YC: Serum insulin-like growth factor (IGF)-I and IGF-binding proteins in lung cancer patients. J Kor Med Sci 14: 401-404, 1999.
5. Cohen P, Peehl DM, Stamey TA, Wilson KF, Clemmons DR and Rosenfeld RG: Elevated levels of insulin-like growth factor-binding protein-2 in the serum of prostate cancer patients. J Clin Endocrinol Metab 76: 1031-1035, 1993.
6. Shariat SF, Lamb DJ, Kattan MW, Nguyen C, Kim J, Beck J, Wheeler TM and Slawin KM: Association of preoperative plasma levels of insulin-like growth factor I and insulin-like growth factor binding proteins-2 and -3 with prostate cancer invasion, progression and metastasis. J Clin Oncol 20: 833-841, 2002.
7. Busund LT, Richardsen E, Busund R, Ukkonen T, Bjørnsen T, Busch C and Stalsberg H: Significant expression of IGFBP2 in breast cancer compared with benign lesions. J Clin Pathol 58: 361-366, 2005.
8. So AI, Levitt RJ, Eigl B, Fazli L, Muramaki M, Leung S, Cheang MC, Nielsen TO, Gleave M and Pollak M: Insulin-like growth factor binding protein-2 is a novel therapeutic target associated with breast cancer. Clin Cancer Res 14: 6944-6954, 2008.
9. Schütt BS, Langkamp M, Rauschnabel U, Ranke MB and Elmlinger MW: Integrin-mediated action of insulin-like growth factor binding protein-2 in tumor cells. J Mol Endocrinol 32: 859-868, 2004.
10. Pereira JJ, Meyer T, Docherty SE, Reid HH, Marshall J, Thompson EW, Rossjohn J and Price JT: Bimolecular interaction of insulin-like growth factor (IGF) binding protein-2 with alphavbeta3 negatively modulates IGF-I-mediated migration and tumor growth. Cancer Res 64: 977-984, 2004.
11. Wang C, Gao C, Meng K, Qiao H and Wang Y: Human adipocytes stimulate invasion of breast cancer MCF-7 cells by secreting IGFBP-2. PLoS One 10: e0119348, 2015.
12. Zaiss AK and Muruve DA: Immunity to adeno-associated virus vectors in animals and humans: A continued challenge. Gene Ther 15: 808-816, 2008.
13. Herzog RW, Yang EY, Couto LB, Hagstrom JN, Elwell D, Fields PA, Burton M, Bellinger DA, Read MS, Brinkhous KM, *et al*: Long-term correction of canine hemophilia B by gene transfer of blood coagulation factor IX mediated by adeno-associated viral vector. Nat Med 5: 56-63, 1999.
14. Wang L, Takabe K, Bidlingmaier SM, Ill CR and Verma IM: Sustained correction of bleeding disorder in hemophilia B mice by gene therapy. Proc Natl Acad Sci USA 96: 3906-3910. 1999.
15. Ponnazhagan S, Mahendra G, Kumar S, Shaw DR, Stockard CR, Grizzle WE and Meleth S: Adeno-associated virus 2-mediated antiangiogenic cancer gene therapy: Long-term efficacy of a vector encoding angiostatin and endostatin over vectors encoding a single factor. Cancer Res 64: 1781-1787, 2004.
16. Collins SA, Buhles A, Scallan MF, Harrison PT, O'Hanlon DM, O'Sullivan GC and Tangney M: AAV2-mediated in vivo immune gene therapy of solid tumours. Genet Vaccines Ther 8: 8, 2010.
17. Alam S, Bowser BS, Conway MJ, Israr M, Tandon A and Meyers C: Adeno-associated virus type 2 infection activates caspase dependent and independent apoptosis in multiple breast cancer lines but not in normal mammary epithelial cells. Mol Cancer 10: 97, 2011.
18. Foulstone EJ, Zeng L, Perks CM and Holly JM: Insulin-like growth factor binding protein 2 (IGFBP-2) promotes growth and survival of breast epithelial cells: Novel regulation of the estrogen receptor. Endocrinology 154: 1780-1793, 2013.
19. Wang C, Bian Z, Wei D and Zhang JG: MiR-29b regulates migration of human breast cancer cells. Mol Cell Biochem 352: 197-207, 2011.
20. Uzoh CC, Holly JM, Biernacka KM, Persad RA, Bahl A, Gillatt D and Perks CM: Insulin-like growth factor-binding protein-2 promotes prostate cancer cell growth via IGF-dependent or -independent mechanisms and reduces the efficacy of docetaxel. Br J Cancer 104: 1587-1593, 2011.
21. Holmes KM, Annala M, Chua CY, Dunlap SM, Liu Y, Hugen N, Moore LM, Cogdell D, Hu L, Nykter M, *et al*: Insulin-like growth factor-binding protein 2-driven glioma progression is prevented by blocking a clinically significant integrin, integrin-linked kinase, and NF-κB network. Proc Natl Acad Sci USA 109: 3475-3480, 2012.
22. Kiepe D, Van Der A, Ciarmatori S, Ständker L, Schütt B, Hoeflich A, Hügel U, Oh J and Tönshoff B: Defined carboxy-terminal fragments of insulin-like growth factor (IGF) binding protein-2 exert similar mitogenic activity on cultured rat growth plate chondrocytes as IGF-I. Endocrinology 149: 4901-4911, 2008.
23. Wang GK, Hu L, Fuller GN and Zhang W: An interaction between insulin-like growth factor-binding protein 2 (IGFBP2) and integrin alpha5 is essential for IGFBP2-induced cell mobility. J Biol Chem 281: 14085-14091, 2006.
24. Sehgal P, Kumar N, Praveen Kumar VR, Patil S, Bhattacharya A, Vijaya Kumar M, Mukherjee G and Kondaiah P: Regulation of protumorigenic pathways by insulin like growth factor binding protein2 and its association along with β-catenin in breast cancer lymph node metastasis. Mol Cancer 12: 63, 2013.
25. Chakrabarty S and Kondratick L: Insulin-like growth factor binding protein-2 stimulates proliferation and activates multiple cascades of the mitogen-activated protein kinase pathways in NIH-OVCAR3 human epithelial ovarian cancer cells. Cancer Biol Ther 5: 189-197, 2006.
26. Chatterjee S, Park ES and Soloff MS: Proliferation of DU145 prostate cancer cells is inhibited by suppressing insulin-like growth factor binding protein-2. Int J Urol 11: 876-884, 2004.
27. Miyake H, Hara I, Yamanaka K, Muramaki M, Gleave M and Eto H: Introduction of insulin-like growth factor binding protein-2 gene into human bladder cancer cells enhances their metastatic potential. Oncol Rep 13: 341-345, 2005.
28. Fukushima T, Tezuka T, Shimomura T, Nakano S and Kataoka H: Silencing of insulin-like growth factor-binding protein-2 in human glioblastoma cells reduces both invasiveness and expression of progression-associated gene CD24. J Biol Chem 282: 18634-18644, 2007.
29. Alam S, Bowser BS, Israr M, Conway MJ and Meyers C: Adeno-associated virus type 2 infection of nude mouse human breast cancer xenograft induces necrotic death and inhibits tumor growth. Cancer Biol Ther 15: 1013-1028, 2014.